Aix * Marseille Université

Project Report
The Connor, Walter and McKown Model

Svetlana Vasileva and Jonathan Arne Tobias Schrohe

1 Introduction

The following Model, published by John A. Connor, David Walter, and Russel McKown in 1977, [2] was developed "to approximate voltage clamp data from repetitive-firing crustacean walking leg axons and activity in response to constant current stimulation" [2].

It is based on the popular Hodgkin and Huxley model [3] developed for squid axons and extends it with ideas from Connor and Stevens [1]. Besides some changed parameters, the key element of this model is a fifth pathway in the electrical circuit model, representing a transient potassium conductance.

2 The Model

The main idea of the Hodgkin and Huxley model is to investigate the electric potential of an axon membrane, resulting from a flow of ions through the membrane's ion channels. It linearizes the ideas of the Goldman-Hodgkin-Katz model for electrodiffusion in the membrane with an electical circuit model.
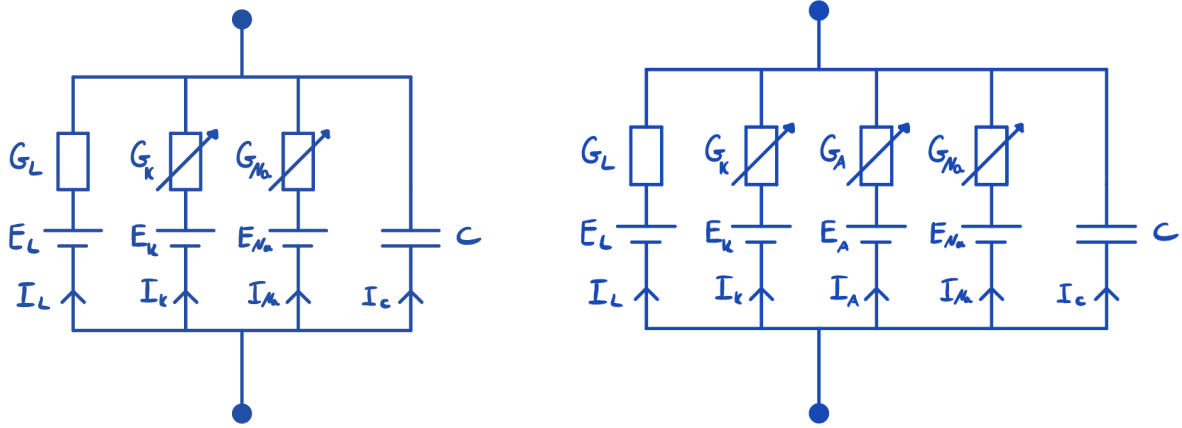
(a) Original Hodgkin and Huxley Model.   (b) Modified model with a fifth branch added.

While a potassium and sodium channel (I_K and I_{Na} respectively) were sufficient for the modelling of the current in a squid axon, the need of a further, transient potassium channel (I_A) for a model of the marine gastropod Anisodoris was found out by Connor and Stevens in a later research study [1]. When trying to model the whole current, the further impact of the phospholipid bilayer (I_C) and the constant leaking current I_L have to be respected as well. Eventually, the total current of the membrane can be described as:

$$I(t) = I_{Na}(t) + I_K(t) + I_A(t) + I_L(t) + I_C(t). \tag{1}$$

The passive, leaking current can be described as:

$$I_L(t) = G_L(V(t) - E_L), \tag{2}$$

where G_L is the leakage conductance, E_L the leakage resting potential and $V(t)$ the electric potential. The phospholipid bilayer that prevents the ions from crossing can be modelled as a capacitive effect

with

$$I_C(t) = C\frac{dV(t)}{dt}. \tag{3}$$

Hodgkin and Huxley described the potassium and sodium ion currents with:

$$I_{Na}(t) = G_{Na}(V(t) - E_{Na}) = \bar{g}_{Na}m^3h(V(t) - E_{Na}), \tag{4}$$

$$I_K(t) = G_K(V(t) - E_K) = \bar{g}_K n^4(V(t) - E_K). \tag{5}$$

They modelled the variable conductances considering that there is a probability for a number of activation gates (m, n) and inactivation gates (h) to open. The gates are opened and closed in the course of time as the membrane potential changes (i.e. $m = m(V(t))$). The asymptotic behaviour of this for infinite times can be visualized in figure 2. The time-course behaviour is modelled in a
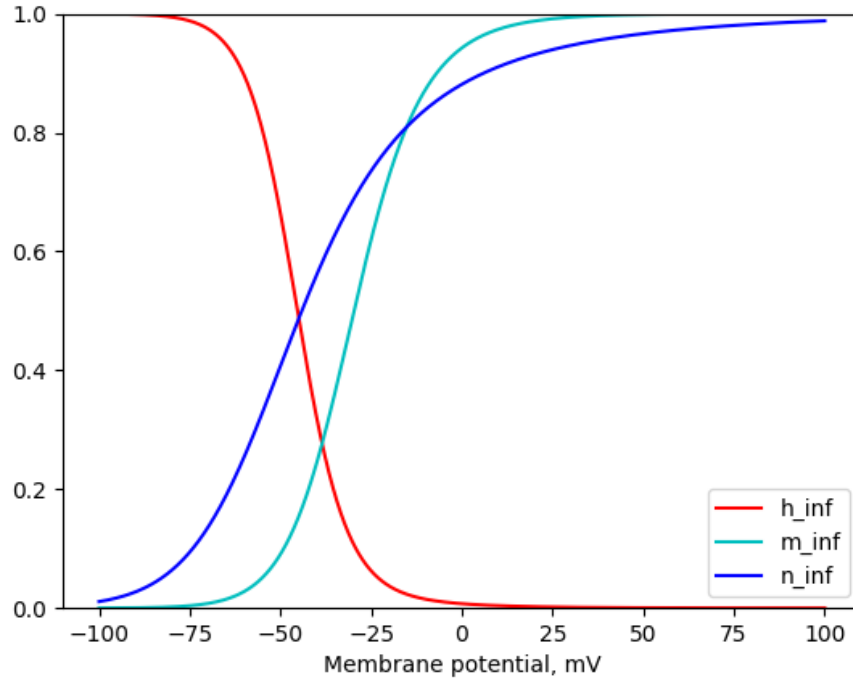

Figure 2: Asymptotic behaviour of channel opening for infinite time.

differential equation (n and h analog):

$$\dot{m} = \alpha_m(V(t))(1 - m) - \beta_m(V(t))m. \tag{6}$$

The transient potassium channels have been modelled in a similar form [1], [2]:

$$I_A(t) = G_A(V(t) - E_A) = \bar{g}_A A^3 B(V(t) - E_A) = \bar{g}_A \left\{ A_\infty(V) \left[1 - e^{-t/\tau_A} \right] \right\}^3 B_\infty(V)[e^{-t/\tau_B}](V(t) - E_A) \tag{7}$$

In this case, the time-course opening behaviour of the channels could be directly explicited in the function $G_A = G(t, V(t))$. Finally, equation (1) can be rearranged to a first order differential equation in $V(t)$, which gives us the full model (equations (8) - (21) and table 1):

It consists of the four differential equations for current

$$
\begin{aligned}
\frac{\mathrm{d}V(t)}{\mathrm{d}t} =& 1/C[I - \bar{g}_{Na}m^3h(V(t) - E_{Na}) - \bar{g}_K n^4(V(t) - E_K) \\
&- \bar{g}_A \left\{ A_\infty(V) \left[1 - e^{-t/\tau_A} \right] \right\}^3 B_\infty(V)[e^{-t/\tau_B}](V(t) - E_A) \\
&- G_L(V(t) - E_L)],
\end{aligned}
\tag{8}
$$

and the first order kinetics for channel opening behaviour

$$
\dot{m} = \alpha_m(V)(1 - m) - \beta_m(V)m, \tag{9}
$$

$$
\dot{h} = \alpha_h(V)(1 - h) - \beta_h(V)h, \tag{10}
$$

$$
\dot{n} = \alpha_n(V)(1 - n) - \beta_n(V)n. \tag{11}
$$

$$
\tag{12}
$$

Furthermore, the following functions are explicited [2]:

$$
\alpha_m = -0.1(V + 35 + \mathrm{MSHFT})/(\exp(-(V + 35 + \mathrm{MSHFT})/10 - 1)), \tag{13}
$$

$$
\beta_m = 4\exp(-(V + 60 + \mathrm{MSHFT})/18), \tag{14}
$$

$$
\alpha_h = 0.07\exp(-(V + 60 + \mathrm{HSHFT})/20), \tag{15}
$$

$$
\alpha_n = -0.01(V + 50 + \mathrm{NSHFT})/(\exp(-(V + 50 + \mathrm{NSHFT})/10) - 1), \tag{16}
$$

$$
\beta_n = 0.125\exp(-(V + 60 + \mathrm{NSHFT})/80), \tag{17}
$$

$$
A_\infty = (0.0761\exp((V + 94.22)/31.84)/(1 + \exp((V + 1.17)/28.93)))^{(1/3)}, \tag{18}
$$

$$
B_\infty = 1/(1 + \exp((V + 53.3)/14.54))^4, \tag{19}
$$

$$
\tau_A = 0.3632 + 1.158/(1 + \exp((V + 55.96)/20.12)), \tag{20}
$$

$$
\tau_B = 1.24 + 2.678/(1 + \exp((V + 50)/16.027)). \tag{21}
$$

The initial condition is:

$$
V(t = 0) = V_0, \tag{22}
$$

$$
m(V(t = 0)) = m_\infty(V_0) = \alpha_m(V_0)/(\alpha_m(V_0) + \beta_m(V_0)), \tag{23}
$$

$$
h(V(t = 0)) = h_\infty(V_0) = \alpha_h(V_0)/(\alpha_h(V_0) + \beta_h(V_0)), \tag{24}
$$

$$
n(V(t = 0)) = n_\infty(V_0) = \alpha_n(V_0)/(\alpha_n(V_0) + \beta_n(V_0)). \tag{25}
$$

The constants are summarized in table 1 [2]:

Table 1: Constants

Constant	Value
E_{Na}	$55\,\mathrm{mV}$
$\bar{g}_{Na}$	$120\,\mathrm{mmho/cm^2}$
E_K	$-72\,\mathrm{mV}$
$\bar{g}_K$	$20\,\mathrm{mmho/cm^2}$
E_A	$-75\,\mathrm{mV}$
$\bar{g}_A$	$47{,}7\,\mathrm{mmho/cm^2}$
E_L	$-17\,\mathrm{mV}$
G_L	$0{,}3\,\mathrm{mmho/cm^2}$
C	$1\,\mathrm{\mu F/cm^2}$
V_0	$-68\,\mathrm{mV}$
MSHFT	$-5{,}3$
HSHFT	-12
NSHFT	$-4{,}3$

Furthermore, the authors set $I = const.$ in their study and examine the behaviour of multiple values for it.

Note that were several typing errors in the publication [2]. The addition and subtraction of 1 in the formulas for α_m and β_h have to be outside of the exponential [3]. Furthermore, the current I_A is calculated with the resting potential E_A, not E_K.

3 Analytical Results

The differential equation together with its initial value forms a Cauchy problem:

$$\begin{cases} \dfrac{\mathrm{d}\boldsymbol{y}(t)}{\mathrm{d}t} = \boldsymbol{f}(t, \boldsymbol{y}(t)), \\ \boldsymbol{y}(t_0) = \boldsymbol{y}_0 \end{cases} \tag{26}$$

where the function $\boldsymbol{f}$ is defined by:

$$\boldsymbol{f}(t, \boldsymbol{y}(t)) = \begin{pmatrix} 1/C \left[I - \displaystyle\sum_{i=\{Na,K,A,L\}} \{G_i(t, V(t)) \cdot (V(t) - E_i)\} \right] \\ \alpha_m(V(t))(1-m) - \beta_m(V(t))m \\ \alpha_h(V(t))(1-h) - \beta_h(V(t))h \\ \alpha_n(V(t))(1-n) - \beta_n(V(t))n \end{pmatrix}, \quad \boldsymbol{y(t)} = \begin{pmatrix} V(t) \\ m(t) \\ h(t) \\ n(t) \end{pmatrix} \tag{27}$$

With view to applying the Cauchy-Lipschitz theorem, we will now regard $\boldsymbol{f}$ as a function $\boldsymbol{f} \colon I \times \Omega \to \mathbb{R}^2$, where $I = \mathbb{R}^+$ and $\Omega = \mathbb{R}^4/(V = \{-35 - \text{MSHFT}, -50 - \text{NSHFT}\})$.

$$\boldsymbol{f}(t, \boldsymbol{y}) = \begin{pmatrix} 1/C \left[I - \sum_{i=\{Na,K,A,L\}} \{G_i(t,V) \cdot (V - E_i)\} \right] \\ \alpha_m(V)(1-m) - \beta_m(V)m \\ \alpha_h(V)(1-h) - \beta_h(V)h \\ \alpha_n(V)(1-n) - \beta_n(V)n \end{pmatrix}, \quad \boldsymbol{y} = \begin{pmatrix} V \\ m \\ h \\ n \end{pmatrix} \tag{28}$$

First, it should be noticed that $\boldsymbol{f}$ is not autonomous due to the presence of $G_A(t, V(t))$, where the time dependency of the channel opening is explicited. $\boldsymbol{f}$ is constructed with compositions between polynomials and exponentials, so $\boldsymbol{f}$ is continuous and differentiable with respect to $(t, \boldsymbol{y})$ on $I \times \Omega$. It should be noticed that the same does not hold for $I \times \mathbb{R}^4$, since α_m and α_n would have a denominator of zero. Now, we apply the Cauchy-Lipschitz Theorem:

$\implies \forall (t_0, \boldsymbol{y}_0) \in I \times \Omega$ the Cauchy problem admits a unique, maximal solution $(I_{max}, \boldsymbol{y})$.

4 Numerical Results

The full model (equations (8) - (21)) was analyzed numerically with the parameters given in table 1. The initial condition was set to $V_0 = -68\,\text{mV}$. The only parameter that remained variable is the current I. The dynamics of the system are studied for different values of this parameter. All the plots show the resting potential. The change of the channel opening is not of major interest and was also not studied in [2].
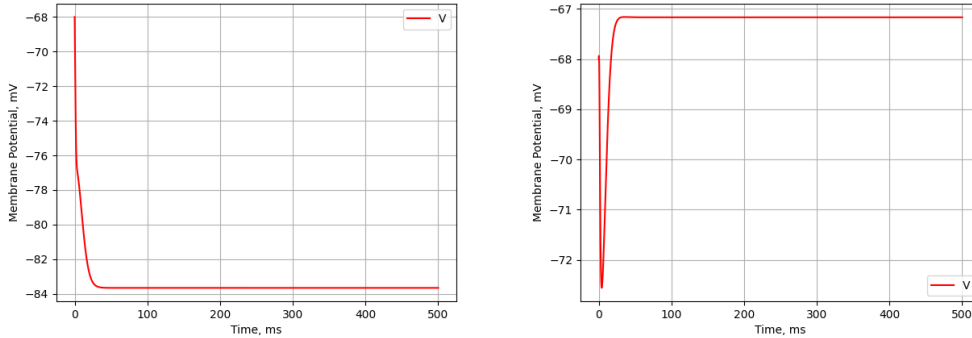

Figure 3: Dynamics of the potential with low current: 1) $I = -20\,\mu\text{A}/\text{cm}^2$ 2) $I = -15\,\mu\text{A}/\text{cm}^2$.

We started analyzing the Potential for a current of $I = -20\,\mu\text{A}/\text{cm}^2$. On this value you can see a strong decay from the original value with an asymptotic behaviour in the end, see figure 5. When increasing the current to $I = -15\,\mu\text{A}/\text{cm}^2$, the Voltage asymptote is lifted to a value above the initial condition. With further increase to $I = -13\,\mu\text{A}/\text{cm}^2$ the growth of a overshoot just before the asymptotic behaviour becomes visible and grows further until a typical peak of a firing neuron appears at around $I = -10\,\mu\text{A}/\text{cm}^2$.

Increasing the current to $I = -8{,}13\,\mu\text{A}/\text{cm}^2$ gives rise to multiple peaks which quickly increase to an ongoing full oscillation at $I = -8{,}12\,\mu\text{A}/\text{cm}^2$. In the paper of Connor [2], this happend at
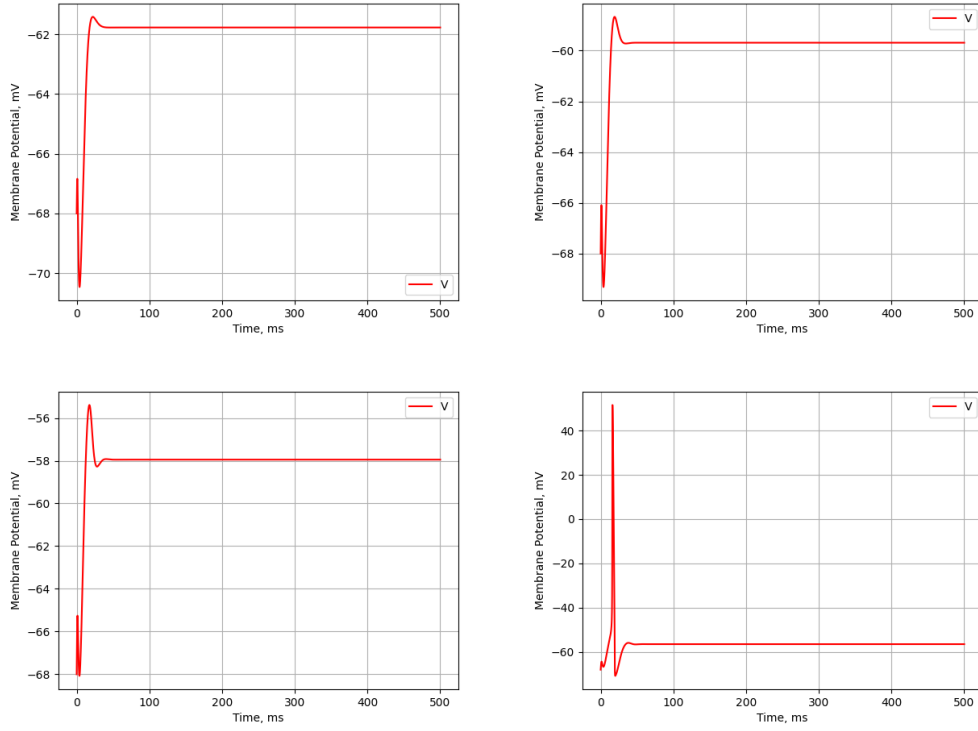
Figure 4: Growing of the first peak with current from -13 to -10: 1) $I = -13\,\mu\text{A}/\text{cm}^2$ 2) $I = -12\,\mu\text{A}/\text{cm}^2$; 3) $I = -11\,\mu\text{A}/\text{cm}^2$; 4) $I = -10\,\mu\text{A}/\text{cm}^2$

$I = 8{,}18\,\mu\text{A}/\text{cm}^2$. Further increase of I mainly increases the frequency of peaks and starts lowering the amplitude as well, like in [2]. All the oscillation show a slight transient in the beginning. While the maximum value is still at $V_{\max} = 50\,\text{mV}$ for $I = 0$, it halves to $V_{\max} = 25\,\text{mV}$ at $I = 80\,\mu\text{A}/\text{cm}^2$. From this point on, the amplitude of the oscillation is strongly damped and vanishes with further increase of I.

In fact, choosing negative currents is questionable but in our case it was the only possibility to show the transition from one peak to periodic behaviour. We were not able to recreate the exact results of [2], but were able to find a qualitatively similar behaviour starting from $I = -8{,}14\,\mu\text{A}/\text{cm}^2$. Nevertheless the recreation of the the low frequencies that Connor and the other Authors were able to simulate was not achieved by us.
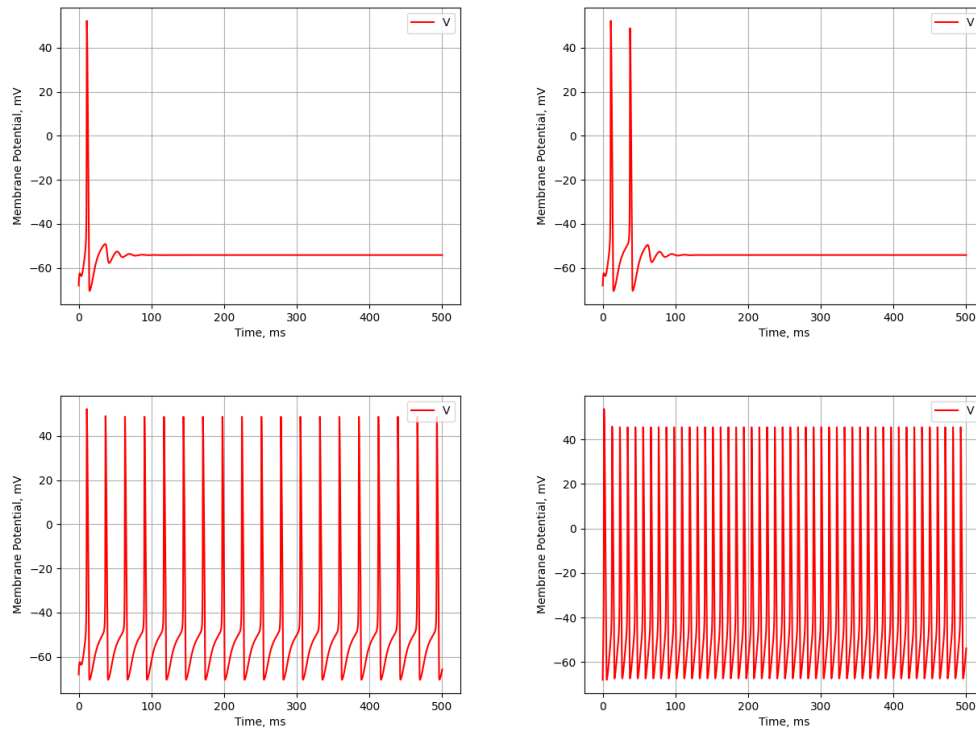
Figure 5: Dynamics of the potential with higher current: 1) $I = -8{,}14\,\mu\mathrm{A/cm}^2$ 2) $I = -8{,}13\,\mu\mathrm{A/cm}^2$; 3) $I = -8{,}12\,\mu\mathrm{A/cm}^2$; 4) $I = 0\,\mu\mathrm{A/cm}^2$

References

[1] J.A. Connor and C. F. Stevens. Voltage clamp studies of a transient outward membrane current in gastropod neural somata. The Journal of Physiology, 213(1):21–30, 1971.

[2] J.A. Connor, D. Walter, and Russel McKown. Neural repetitive firing: Modifications of the hodgkin-huxley axon suggested by experimental results from crustacean axons. Biophysical Journal, 18(1):81–102, 1977.

[3] A.L. Hodkin and A. F. Huxley. A quantitative description of membrane current and its application to conduction and excitation in nerve. The Journal of Physiology, 117(4):500–544, 1952.